On the Degrees of Freedom of Interference Broadcast Channels with Topological Interference Management

On the Degrees of Freedom of Interference Broadcast Channels with Topological Interference Management

Paula Aquilina, *Student Member, IEEE,* and Tharmalingam Ratnarajah, *Senior Member, IEEE*

***Abstract*—Topological interference management is the study of achievable rates within communication networks with no channel state information at the transmitter (CSIT) beyond knowledge of the network structure itself. In this work we study the degrees of freedom (DoF) of a two-cell two-user-per-cell interference broadcast channel (IBC) with alternating connectivity and global topological interference management. The topological information allows transmitters to track the changing network topology and exploit the varying connectivity states to achieve a DoF gain. We derive novel DoF outer bounds for the two-cell two-user-per-cell IBC with alternating connectivity. This analysis is carried out for different system configurations, namely, single-input single-output (SISO), multiple-input single-output (MISO) and multiple-input multiple-output (MIMO) systems. While global channel knowledge is always restricted to topological information only, we introduce a mixed CSIT setting where varying degrees of local CSIT availability are considered depending on the system configuration. Additionally, we investigate the achievability of the derived bounds and propose new transmission schemes based on joint coding across states. Results show that DoF higher than those conventionally obtained without global topological information are achievable, indicating that even such a minimal level of global CSIT is still highly useful.**

***Index Terms*—Alternating connectivity, degrees of freedom, interference broadcast channel, topological interference management.**

I. Introduction

In recent years major advances have been made in terms of understanding the information-theoretic capacity limits of interference limited networks. Results indicate that the maximum achievable capacity is higher than what is currently obtained via the use of conventional techniques, primarily under the assumption of abundant and accurate channel state information at the transmitter (CSIT). While this has given rise to a number of innovative ways on how to exploit different aspects of CSIT, the theoretical gains have been difficult to translate into practical ones due to the idealistic CSIT requirements. Therefore moving on from the initial perfect CSIT studies [1], [2], the current research direction is to focus on more relaxed assumptions in order to reach a compromise where higher rates can be achieved in realistic CSIT settings.

Within the context of relaxed CSIT, various situations have been considered in literature. Some works rely on specific properties of the channel links themselves, for example CSIT that consists of specific coherence patterns that are either naturally occurring [3] or enforced [4], and compound channels [5] where the channel realisations come from a finite set of possibilities. Other works focus on using the available CSIT even though it is not perfect. For example [6] and [7] show that even completely delayed CSIT provides a gain in achievable degrees of freedom (DoF). Scenarios with both delayed and imperfect current CSIT are considered in [8] and [9]. A combined setting where the CSIT alternates between perfect, delayed and unavailable is analysed in [10]. Literature mentioned so far assumes all transmitters have an identical view of the network; however this is not always a prerequisite. For example, in [11] transmitters only have perfect CSIT for a restricted subset of the global channel links, with this subset being specific to each transmitter. Additionally, situations where nodes have asymmetric local views of the global network structure are also considered in [12].

A new but complementary perspective to interference management was introduced in [13]. Rather than starting with abundant CSIT and then moving into more relaxed scenarios, it considers the issue from the opposite end of the spectrum with no CSIT except for knowledge of the network's topological structure. This approach is known as topological interference management, and provides a unified view of linear wired and wireless networks. A main advantage is the minimal CSIT requirement; a single bit per link is enough to indicate whether the link is present or not. The work in [14] considers a similar problem but for the case where transmitters cooperate via message sharing; results show that considerable DoF gains can be obtained for networks that are not fully connected.

Throughout the studies in [13] and [14] it is assumed that network topology is fixed for the duration of communication. In this work, we move beyond this limitation and consider a scenario where inter-cell connectivity may vary in order to analyse the DoF gains that can be achieved. The overall setting is referred to as an alternating connectivity scenario and was also considered for the two-user single-input single-output (SISO) interference channel (IC) and the X channel in [15], and three-user SISO ICs with various restrictions in [16] and [17]. Here we focus on the more complex interference broadcast channel (IBC), which has the additional challenge

This work was supported by the UK Engineering and Physical Sciences Research Council (EPSRC) under grant number EP/L025299/1. The work of P. Aquilina was also supported by the Seventh Framework Programme for Research of the European Commission under grant number HARP-318489 and ADEL-619647. A preliminary version of this work was presented in part at ICASSP 2015 and ISIT 2015.

P. Aquilina and T. Ratnarajah are with the Institute of Digital Communications, School of Engineering, The University of Edinburgh, Alexander Graham Bell Building, Kings Buildings, Mayfield Road, Edinburgh, EH9 3JL, United Kingdom. (email: {p.aquilina, t.ratnarajah}@ed.ac.uk).

of intra-cell interference, and also introduce a mixed CSIT setting where global topological knowledge is combined with varying degrees of local CSIT.

The main contribution of this work is in the derivation of novel DoF outer bounds for the two-cell two-user-per-cell IBC with alternating connectivity. While our initial focus is on a SISO system, we also consider multiple-input single-output (MISO) and multiple-input multiple-output (MIMO) configurations as a means of resolving intra-cell interference. Global channel knowledge is restricted to topological information only; however local CSIT availability varies depending on the system configuration itself, leading to a mixed CSIT setting for the MISO case. The achievability of the derived bounds is investigated for a variety of contexts. Results show that DoF higher than those conventionally obtained without global topological knowledge can be achieved, proving that even such a minimal level of global CSIT is still very useful. In particular, for all system configurations we show how the bounds are tight and achievable when a single state has a probability of occurrence equal to one. Additionally, we propose novel transmission schemes based on joint coding across states that are applicable for arbitrary state probabilities and analyse their performance, both for the general case and for situations where all states are equiprobable.

The rest of this paper is organised as follows. Section II provides the problem setting by introducing the system model, the alternating connectivity scenario, and the local CSIT availability. Next, in Section III we present the DoF outer bound for the SISO system and give an overview of its derivation, while the MISO and MIMO counterpart is provided in Section IV. The achievability of the derived DoF outer bounds is investigated in Section V and Section VI respectively. Section VII shows how the wireless network DoF results can be applied as capacity results for the corresponding wired network instances. Finally, Section VIII provides some concluding remarks. Additionally, there are three appendices which provide extra details required to complete the outer bound derivations.

II. Problem Setting

We consider the two-cell two-user-per cell IBC. This consists of two adjacent cells in a wireless network, where the first cell includes base station (BS) A and receivers $a1$ and $a2$, while the second cell has BS B and receivers $b1$ and $b2$. The basic network structure is shown in Fig. 1, where inter-cell interference links are omitted and the solid lines represent useful links over which the desired symbols are delivered.

The general input-output relationship is given by,

$$Y^r[n] = H_{r,A}[n]X^A[n] + H_{r,B}[n]X^B[n] + Z^r[n] \quad (1)$$

where at channel use index $[n]$, $Y^r[n]$ is the signal observed at receiver r for $r \in \{a1, a2, b1, b2\}$, $X^C[n]$ is the signal sent from transmitter C for $C \in \{A, B\}$, $Z^r[n]$ represents unit variance additive white Gaussian noise (AWGN) at receiver r and $H_{r,C}[n]$ is the channel link between transmitter C and receiver r whose entries are i.i.d. and drawn from a continuous distribution. Additionally $\mathbb{E}(\|X^C[n]\|^2) \leq P$,

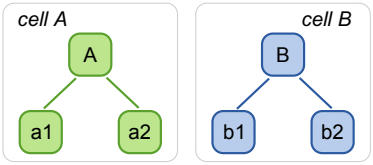

Fig. 1: Two-cell two-user-per-cell network with omitted inter-cell interference links.

where P represents the transmit power constraint and is equal to the signal-to-noise ratio (SNR) for unit power AWGN. Note that for notational simplicity the channel use index $[n]$ will be omitted throughout the rest of this work. Also, since all noise terms are drawn from the same distribution, they are all statistically equivalent, therefore we will use the general notation Z throughout.

Within this setting, inter-cell interference can occur between any of the users and the non-corresponding BS. We consider an alternating connectivity scenario where inter-cell connectivity is not fixed throughout the duration of the whole communication process. Connectivity can easily vary in wireless networks, where some links may go into deep fade making them effectively non-existent. Additionally, in frequency selective environments, frequency hopping or multi-carrier transmission may also create a variety of inter-cell connectivity states. For the scenario considered in this work, a total of 16 different connectivity states may occur, as shown in Fig. 2 at the top of the following page. Each of these states is associated with a probability of occurrence λ_k for $k = 1, \ldots, 16$, where $\sum_{k=1}^{16} \lambda_k = 1$. Note that to ensure the problem is non-degenerate, desired links are considered to be always present and able to support a desired rate in the absence of interference.

For each cell, define M as the number of antennas at the BS and N as the number of antennas at each of the two receivers. With an appropriate choice of M and N, spatial multiplexing can be applied within the cells to resolve intra-cell interference such that each BS can simultaneously deliver one symbol to its corresponding two users, thereby achieving 2 DoF per cell provided no inter-cell interference is present.

For a mixed CSIT[1] setting, where in addition to global topological CSIT perfect current local CSIT is also available, in the absence of inter-cell interference, achievable DoF per cell are given by $\min\{M, KN\}$ [19], where K represents the number of users in each cell. This paper considers a scenario where each cell has two users, thus any $M \times 1$ system (where for MISO $M \geq 2$ by definition) achieves the required 2 DoF per cell. This is possible via zero-forcing (ZF) precoding. Consider a general cell C having users $c1$ and $c2$, where BS C transmits a combined symbol, X^C, consisting of s_{c1} intended for user $c1$ and s_{c2} intended for user $c2$. Given the availability of local CSIT, s_{c_1} can be precoded such that it is orthogonal to the channel from BS C to user $c2$ and s_{c2} can be precoded such that it is orthogonal to the channel from BS C to user $c1$. This allows users to extract their desired symbol from a single

[1]Throughout this work the term *mixed CSIT* is used to refer to a mixture of global topological information and perfect current local CSIT. This is different to prior usage of the term in [8] and [18], where it is used to refer to a mixture of perfect delayed CSIT and imperfect current CSIT.

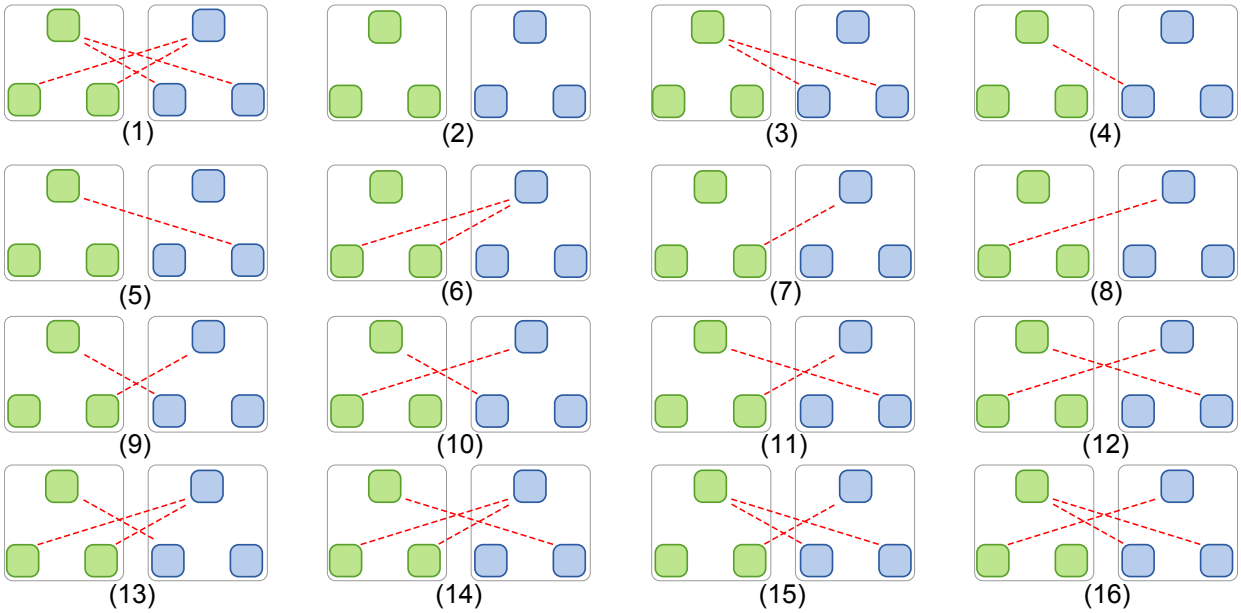

Fig. 2: Set of all possible inter-cell connectivity states for the two-cell two-user-per-cell IBC. Cell A transmitters and receivers are on the left in green, while cell B elements are on the right in blue. The dashed red lines represent the interference links.

observation of X^C, thereby achieving 2 DOF within that cell if no inter-cell interference is present.

On the other hand, if local CSIT is not available, in the absence of inter-cell interference achievable DoF per cell are equal to $\min\{M, N\}$ [20]. Therefore any $M\times 2$ MIMO system (where by definition for MIMO $M \geq 2$), can achieve the required 2 DoF per cell. The same DoF can also be achieved by any $2 \times N$ MIMO system (where $N \geq 2$ by definition). Consider a general cell C having users $c1$ and $c2$, where the BS transmits a combined symbol, X^C, consisting of s_{c1} and s_{c2}, and the antenna configuration is either $M \times 2$ or $2 \times N$. Due to the multiple antenna setting, each user can obtain two independent equations for the two unknown symbols and can therefore decode for the desired one. This results in achievable DoF of 2 per cell if no inter-cell interference is present.

Note that for the SISO scenario spatial multiplexing is not an option, since by definition $M = N = 1$; thereby only 1 DoF per cell can be achieved.

Regardless of the system configuration, if no feedback is available with respect to the alternating global network topology, both transmitters have to assume full inter-cell connectivity throughout, i.e. State 1 in Fig. 2. This only allows for one possible transmission strategy, where BS A and BS B are provided with non-overlapping transmission opportunities and leads to a sum DoF across the two cells of 1 for the SISO configuration and 2 for the MISO system with local CSIT or the MIMO one without local CSIT. Considering all the states in Fig. 2, it is clear that assuming full connectivity throughout is wasteful in terms of network resource use. States 2 to 16 have a smaller amount of inter-cell interference and may potentially achieve higher sum DoF than the fully connected scenario in state 1.

Our interest lies in exploiting this opportunity whilst keeping the global CSIT requirement to a minimum. Therefore while varying degrees of local CSIT are considered, global CSIT is always restricted to topological information only. This requires just 1 bit of CSIT per inter-cell interference link, used to indicate whether interference may be experienced over that link or not. Similar to the setup in [13], power received over an undesired link is compared to a pre-established threshold value equal to the noise floor. If received power is below the threshold, then the link is considered weak and effectively non-existent, and a zero is assigned to the corresponding bit. On the other hand, a one is assigned to links for which the received power is above the noise floor; this indicates a strong link over which significant interference is experienced.

While the setting described so far is sufficient to analyse the MISO and MIMO IBC systems presented in this section, within this work we also consider a SISO scenario which requires further reformulation. For SISO systems maximum achievable DoF per cell equal to 1 can be achieved simply by avoiding intra-cell interference and serving only one user at a time. Hence, from a DoF outer bound perspective, we can consider the case where for every instant each BS selects one user to be its designated user to serve, according to what is most advantageous in terms of achievable sum rate. Define U as the cell A designated user i.e. $U \in \{a1, a2\}$ and V as the cell B designated user i.e. $V \in \{b1, b2\}$. For any given U and V, the original network in Fig. 1 can be represented by the equivalent one in Fig. 3, where only four (U, V) combinations may occur, i.e.

$$(U, V) \in \{\ (a1, b1),\ (a2, b1),\ (a1, b2),\ (a2, b2)\ \}\ . \qquad (2)$$

Having defined an equivalent network for the SISO scenario, the set of 16 alternating states from Fig. 2 can be mapped to a reduced set of only 4 possible states, as in Fig. 4 on the following page. For any given (U, V) combination it only matters whether inter-cell interference affects the designated users. For example, when $(U, V) = (a1, b1)$ in state 9 from Fig. 2, $a1$ is free from inter-cell interference while b_1 receives interference from BS A; thus from the perspective of this particular (U, V) combination, state 9 corresponds to state

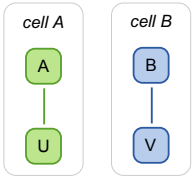

Fig. 3: Equivalent network for SISO scenario, where U represents the cell A designated user and V represents the cell B designated user.

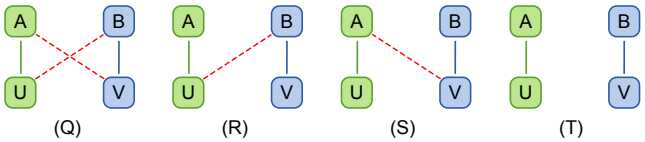

Fig. 4: Reduced set of states used to replace original ones from Fig. 2 when considering the equivalent network for the SISO scenario in Fig. 3.

S in Fig. 4. Next, consider state 9 from the perspective of $(U, V) = (a1, b2)$. In this case both $a1$ and $b2$ are free from inter-cell interference, hence state 9 is mapped to the no interference state T in Fig. 4. Similar arguments can be made for all (U, V) combinations listed in (2) and all the states depicted in Fig. 2. The mapping of the original set of states to the reduced one for each (U, V) combination is provided in Table I.

TABLE I: Mapping of original states from Fig. 2 to the equivalent reduced set in Fig. 4 for each possible (U, V) combination.

$(\mathbf{U}, \mathbf{V})$	$\mathbf{Q}$	$\mathbf{R}$	$\mathbf{S}$	$\mathbf{T}$
$(a1, b1)$	$1, 10, 13, 16$	$6, 8, 12, 14$	$3, 4, 9, 15$	$2, 5, 7, 11$
$(a2, b1)$	$1, 9, 13, 15$	$6, 7, 11, 14$	$3, 4, 10, 16$	$2, 5, 8, 12$
$(a1, b2)$	$1, 12, 14, 16$	$6, 8, 10, 13$	$3, 5, 11, 15$	$2, 4, 7, 9$
$(a2, b2)$	$1, 11, 14, 15$	$6, 7, 9, 13$	$3, 5, 12, 16$	$2, 4, 8, 10$

III. DOF OUTER BOUND FOR SISO IBC

In this section we present a DoF outer bound for the two-cell two-user-per-cell SISO IBC with alternating connectivity.

Theorem 1: For the two-cell two-user-per-cell SISO IBC with alternating connectivity, the sum DoF, $d_{\Sigma,S}$, can be characterised as

$$d_{\Sigma,S} \leq 2 - \Theta$$

where

$$\Theta = \max \begin{cases} \lambda_3 + \lambda_6 \\ \lambda_1 + \lambda_6 + \lambda_{13} + \lambda_{14} \\ \lambda_1 + \lambda_3 + \lambda_{15} + \lambda_{16} \, . \end{cases} \tag{3}$$

Proof:

The overall outer bound consists of merging together bounds originating from different sources; one comes from the summation of the achievable rates per cell and an additional pair arises from genie aided bounds for each cell. In this section we present an abbreviated version of the proof showing how the cell A expressions are obtained, details for their cell B counterparts are provided in Appendix A.

A. Sum bound

For the sum bound, first we obtain separate expressions for the achievable rate within each cell, these are then combined to give an overall outer bound for the sum DoF across the two cells. Starting with the cell A achievable rate, we have

$$nR_A \leq I(W^A; Y_1^U, \ldots, Y_{16}^U) + n\epsilon \tag{4}$$

where W^A is the message set from BS A and Y_k^U is the signal received by the cell A designated user U during state k. (4) can be further expressed as

$$\begin{aligned} nR_A &\leq h(Y_1^U, \ldots, Y_{16}^U) - h(Y_1^U, \ldots, Y_{16}^U \mid W^A) + n\epsilon \\ &\overset{(a)}{=} h(Y_1^U, \ldots, Y_{16}^U) - h(Y_Q^U, Y_R^U, Y_S^U, Y_T^U \mid W^A) + n\epsilon \\ &= h(Y_1^U, \ldots, Y_{16}^U) - h(Y_R^U, Y_S^U, Y_T^U \mid W^A) \\ &\quad - \underbrace{h(Y_Q^U \mid W^A, Y_R^U, Y_S^U, Y_T^U)}_{\geq h(Y_Q^U \mid W^A, Y_R^U, Y_S^U, Y_T^U, W^B) = no(\log P)} + n\epsilon \\ &\overset{(b)}{\leq} h(Y_1^U, \ldots, Y_{16}^U) \\ &\quad - h(Y_R^U, Y_S^U, Y_T^U \mid W^A) + no(\log P) + n\epsilon \end{aligned} \tag{5}$$

where (a) follows since the original set of 16 states are all contained within states Q, R, S and T for the equivalent SISO scenario, and (b) follows since conditioning reduces entropy and the effect of noise disappears at high SNR. Note that $o(\cdot)$ comes from the standard Landau notation, where $f(x) = o(g(x))$ implies $\lim_{x\to\infty} f(x)/g(x) = 0$.

Considering (5) and the state configurations in Fig. 4, it can be noticed that the received signal for the cell A designated user U in states S and T consists only of an X^A component and noise. The X^A component has no effect on entropy since it is solely a function of W^A, while the effect of noise disappears as $P \to \infty$ and can be integrated into the $no(\log P)$ term, resulting in

$$nR_A \leq h(Y_1^U, \ldots, Y_{16}^U) - h(Y_R^U \mid W^A) + no(\log P) + n\epsilon. \tag{6}$$

For all states corresponding to R, the cell A received signal is combination of X^A, X^B and noise. The X^A component is negligible with respect to entropy. The X^B and noise components are independent of W^A. Additionally, since $H_{U,B}$ and $H_{V,B}$ are independently drawn from the same distribution, they are statistically equivalent and interchangeable [20]. Therefore the X^B and noise terms can be represented by the signal received at the cell B designated user V, provided that V itself has no inter-cell interference. Comparing the list of all R states from Table I, it can be noticed that this substitution is guaranteed as being always possible regardless of the current (U, V) combination only for state 6. Using this information, the cell A rate outer bound from (6) can be expressed as

$$\begin{aligned} nR_A \leq\ & h(Y_1^U, \ldots, Y_{16}^U) + no(\log P) + n\epsilon \\ & - h(H_{U,A} X_6^A + H_{U,B} X_6^B + Z \mid W^A) \\ =\ & h(Y_1^U, \ldots, Y_{16}^U) - h(H_{V,B} X_6^B + Z) + no(\log P) + n\epsilon \\ =\ & h(Y_1^U, \ldots, Y_{16}^U) - h(Y_6^V) + no(\log P) + n\epsilon \\ \leq\ & h(Y_1^U) + \cdots + h(Y_{16}^U) - h(Y_6^V) + no(\log P) + n\epsilon \, . \end{aligned} \tag{7}$$

Following a similar process from the perspective of cell B, we obtain the cell B rate outer bound as (8) below. Additional details on how to derive this expression are provided in Appendix A-I.

$$nR_B \leq h(Y_1^V) + \cdots + h(Y_{16}^V) - h(Y_3^U) + no(\log P) + n\epsilon. \tag{8}$$

$$nR_{\Sigma(SB)} \leq h(Y_1^U)+h(Y_2^U)+h(Y_4^U)+\cdots+h(Y_{16}^U)+h(Y_1^V)+\cdots+h(Y_5^V)+h(Y_7^V)+\cdots+h(Y_{16}^V)+no(\log P)+n\epsilon$$
$$\overset{(a)}{\leq} n\,(\,\lambda_1+\lambda_2+\lambda_4+\cdots+\lambda_{16}+\lambda_1+\cdots+\lambda_5+\lambda_7+\cdots+\lambda_{16}\,)(\log P)+no(\log P)+n\epsilon \quad (9)$$

$$nR_{\Sigma(GA)} \leq h(Y_1^U,\ldots,Y_{16}^U,G^A) - \underbrace{h(Y_1^U,\ldots,Y_{16}^U,G^A \mid W^A,W^B)}_{=no(\log P)}+n\epsilon$$
$$\leq h(Y_1^U)+\cdots+h(Y_{16}^U)+h(Y_2^V)+\cdots+h(Y_5^V)+h(Y_7^V)+\cdots+h(Y_{12}^V)+h(Y_{15}^V)+h(Y_{16}^V)+no(\log P)+n\epsilon$$
$$\overset{(a)}{\leq} n\,(\,1+\lambda_2+\cdots+\lambda_5+\lambda_7+\cdots+\lambda_{12}+\lambda_{15}+\lambda_{16}\,)(\log P)+no(\log P)+n\epsilon$$
$$\overset{(b)}{=} n\,(\,2-\lambda_1-\lambda_6-\lambda_{13}-\lambda_{14}\,)(\log P)+no(\log P)+n\epsilon \quad (12)$$

The separate expressions in (7) and (8) are combined together as $nR_{\Sigma(SB)} = nR_A + nR_B$ to obtain an outer bound for the achievable rate across the whole network as in (9), at the top of this page, where λ_k represents the probability of occurrence of the corresponding state k and reflects the effect of alternating connectivity, and (a) follows from the fact that Gaussian distribution maximises differential entropy. Applying $\sum_{k=1}^{16}\lambda_k = 1$ to (9), we obtain

$$nR_{\Sigma(SB)} \leq n(2-\lambda_3-\lambda_6)(\log P)+no(\log P)+n\epsilon\,.$$

Normalising by $n(\log P)$ and letting $P\to\infty$, results in

$$d_{\Sigma(SB)} \leq 2-\lambda_3-\lambda_6\,. \quad (10)$$

B. Genie aided bounds

Genie aided bounds are obtained by finding an outer bound on the rate achievable at a single cell after providing it with enough extra information, i.e. 'genies', such that the data required across the two cells can be decoded within that cell.

Starting with the genie aided bound for cell A, we have

$$nR_{\Sigma(GA)} \leq I(W^A,W^B;Y_1^U,\ldots,Y_{16}^U,G^A)+n\epsilon \quad (11)$$

where G^A represents the genie set required by cell A. Genies are necessary in cases where no cell B data is received at cell A, thus G^A consists of all the original states from Fig. 2 that correspond to states S and T in Fig. 4. Considering the corresponding entries from Table I, we obtain

$$G^A = \{Y_2^V,\ldots,Y_5^V,Y_7^V,\ldots,Y_{12}^V,Y_{15}^V,Y_{16}^V\}.$$

Having defined G^A, the initial expression in (11) can be represented as (12) at the top of this page, where (a) follows from the fact that Gaussian distribution maximises differential entropy and (b) follows from the fact that $\sum_{k=1}^{16}\lambda_k = 1$. Normalising by $n(\log P)$ and letting $P\to\infty$, we have

$$d_{\Sigma(GA)} \leq 2-\lambda_1-\lambda_6-\lambda_{13}-\lambda_{14}\,. \quad (13)$$

Following a similar process for cell B, details for which can be found in Appendix A-II, we obtain the cell B genie aided outer bound as in (14) below.

$$d_{\Sigma(GB)} \leq\ 2-\lambda_1-\lambda_3-\lambda_{15}-\lambda_{16} \quad (14)$$

Finally the result for $d_{\Sigma,S}$ in Theorem 1 is obtained by combining the separate bounds from (10), (13) and (14). ■

IV. DOF OUTER BOUND FOR MISO AND MIMO IBC

As outlined in Section II, a MISO system with local CSIT and $M \geq 2$ transmit antennas achieves 2 DoF per cell provided there is no inter-cell interference. Similarly a MIMO system with no local CSIT having either $M = 2$ and $N \geq 2$ or $M \geq 2$ and $N = 2$ can also achieve 2 DoF per cell. This makes the two settings equivalent from an achievable DoF perspective, since both apply spatial multiplexing to resolve intra-cell interference. Based on this equivalence, it follows that the same outer bound applies to both cases. Therefore in this section we present a DoF outer bound for two-cell two-user-per-cell MISO/MIMO IBC systems which handle intra-cell interference via spatial multiplexing.

Theorem 2: For the two-cell two-user-per-cell MISO/ MIMO IBC with alternating connectivity, where intra-cell interference is handled via spatial multiplexing, the sum DoF, $d_{\Sigma,M}$, can be characterised as

$$d_{\Sigma,M} \leq 2+2\lambda_2+\lambda_4+\lambda_5+\lambda_7+\lambda_8+\Phi$$

where

$$\Phi = \min\begin{cases} 2\lambda_1 \\ 2\lambda_3+\lambda_4+\lambda_5+\lambda_9+\cdots+\lambda_{12}+\lambda_{15}+\lambda_{16} \\ 2\lambda_6+\lambda_7+\cdots+\lambda_{14}\,. \end{cases} \quad (15)$$

Proof:

To obtain the overall outer bound, bounds originating from different sources are merged together; one comes from the summation of outer bounds for the achievable rate at each user and another two arise from genie aided bounds obtained on a per cell basis. Due to the length of the proof itself, we only present an abbreviated version in this section; additional details are provided in Appendix B.

A. Sum bound

To obtain the sum DoF outer bound, we require separate expressions for the achievable rate at each user, which are then combined together. Starting with the achievable rate at user $a1$, we have

$$nR_{a1} \leq I(W^A;Y_1^{a1},\ldots,Y_{16}^{a1})+\ n\epsilon$$

where W^A is the message set from BS A and Y_k^{a1} is the signal received by user $a1$ during state k. This can be further represented as

$$nR_{a1} \leq h(Y_1^{a1},\ldots,Y_{16}^{a1}) - h(Y_1^{a1},\ldots,Y_{16}^{a1} \mid W^A)+\ n\epsilon$$

$$
\begin{aligned}
nR_{a1} &\leq h(Y_1^{a1},\ldots,Y_{16}^{a1}) - h(Y_{\Delta}^{a1} \mid W^A) - E_{a1} + no(\log P) + n\epsilon \\
&\overset{(a)}{=} h(Y_1^{a1},\ldots,Y_{16}^{a1}) - h(H_{a1,A}X_6^A + H_{a1,B}X_6^B + Z,\ldots,H_{a1,A}X_{14}^A + H_{a1,B}X_{14}^B + Z \mid W^A) - E_{a1} + no(\log P) + n\epsilon \\
&\overset{(b)}{=} h(Y_1^{a1},\ldots,Y_{16}^{a1}) - h(H_{a1,B}X_6^B + Z, H_{a1,B}X_8^B + Z, H_{a1,B}X_{10}^B + Z, H_{a1,B}X_{12}^B + Z, H_{a1,B}X_{13}^B + Z, H_{a1,B}X_{14}^B + Z) \\
&\quad - E_{a1} + no(\log P) + n\epsilon \\
&\overset{(c)}{=} h(Y_1^{a1},\ldots,Y_{16}^{a1}) - h(H_{b2,B}X_6^B + Z, H_{b1,B}X_8^B + Z, H_{b2,B}X_{10}^B + Z, H_{b1,B}X_{12}^B + Z, H_{b2,B}X_{13}^B + Z, H_{b1,B}X_{14}^B + Z) \\
&\quad - E_{a1} + no(\log P) + n\epsilon \\
&\overset{(d)}{=} h(Y_1^{a1},\ldots,Y_{16}^{a1}) - h(Y_6^{b2}, Y_8^{b1}, Y_{10}^{b2}, Y_{12}^{b1}, Y_{13}^{b2}, Y_{14}^{b1}) - E_{a1} + no(\log P) + n\epsilon
\end{aligned} \tag{17}
$$

$$nR_{a1} \leq h(Y_1^{a1}) + \cdots + h(Y_{16}^{a1}) - h(Y_6^{b2}) - h(Y_8^{b1}) - h(Y_{10}^{b2}) - h(Y_{12}^{b1}) - h(Y_{13}^{b2}) - h(Y_{14}^{b1}) - E_{a1} + no(\log P) + n\epsilon \tag{18}$$

$$nR_{a2} \leq h(Y_1^{a2}) + \cdots + h(Y_{16}^{a2}) - h(Y_6^{b1}) - h(Y_7^{b2}) - h(Y_9^{b2}) - h(Y_{11}^{b1}) - h(Y_{13}^{b2}) - h(Y_{14}^{b1}) - E_{a2} + no(\log P) + n\epsilon \tag{19}$$

$$nR_{b1} \leq h(Y_1^{b1}) + \cdots + h(Y_{16}^{b1}) - h(Y_3^{a1}) - h(Y_4^{a1}) - h(Y_9^{a1}) - h(Y_{10}^{a2}) - h(Y_{15}^{a1}) - h(Y_{16}^{a2}) - E_{b1} + no(\log P) + n\epsilon \tag{20}$$

$$nR_{b2} \leq h(Y_1^{b2}) + \cdots + h(Y_{16}^{b2}) - h(Y_3^{a2}) - h(Y_5^{a2}) - h(Y_{11}^{a1}) - h(Y_{12}^{a2}) - h(Y_{15}^{a1}) - h(Y_{16}^{a2}) - E_{b2} + no(\log P) + n\epsilon \tag{21}$$

$$
\begin{aligned}
nR_{\Sigma(SB)} \leq\ & h(Y_1^{a1}) + h(Y_2^{a1}) + h(Y_5^{a1}) + \cdots + h(Y_8^{a1}) + h(Y_{10}^{a1}) + h(Y_{12}^{a1}) + h(Y_{13}^{a1}) + h(Y_{14}^{a1}) + h(Y_{16}^{a1}) + h(Y_1^{a2}) \\
&+ h(Y_2^{a2}) + h(Y_4^{a2}) + h(Y_6^{a2}) + \cdots + h(Y_9^{a2}) + h(Y_{11}^{a2}) + h(Y_{13}^{a2}) + h(Y_{14}^{a2}) + h(Y_{15}^{a2}) + h(Y_7^{b1}) + h(Y_9^{b1}) \\
&+ h(Y_1^{b1}) + \cdots + h(Y_5^{b1}) + h(Y_{10}^{b1}) + h(Y_{13}^{b1}) + h(Y_{15}^{b1}) + h(Y_{16}^{b1}) + h(Y_1^{b2}) + \cdots + h(Y_5^{b2}) + h(Y_8^{b2}) + h(Y_{11}^{b2}) \\
&+ h(Y_{12}^{b2}) + h(Y_{14}^{b2}) + h(Y_{15}^{b2}) + h(Y_{16}^{b2}) - h(Y_{15}^{a1}) - h(Y_{16}^{a2}) - h(Y_{14}^{b1}) - h(Y_{13}^{b2}) - E_{a1} - E_{a2} - E_{b1} - E_{b2} \\
&+ no(\log P) + n\epsilon
\end{aligned} \tag{22}
$$

$$
\begin{aligned}
&= h(Y_1^{a1},\ldots,Y_{16}^{a1}) - h(Y_2^{a1},\ldots,Y_{15}^{a1} \mid W^A) \\
&\quad - \underbrace{h(Y_1^{a1}, Y_{16}^{a1} \mid W^A, Y_2^{a1},\ldots,Y_{15}^{a1})}_{=E_{a1}} + n\epsilon\,.
\end{aligned} \tag{16}
$$

Next it can be observed that $Y_2^{a1},\ldots,Y_{15}^{a1}$ can be divided into two sets, as follows

$$\Delta' = \{2,3,4,5,7,9,11,15\} \text{ and } \Delta = \{6,8,10,12,13,14\}$$

where for the Δ' set signals received at $a1$ consist only of an X^A component, which has no effect on entropy, and noise, whose contribution can be represented as $no(\log P)$. For the Δ set, data received at $a1$ is a combination of X^A, X^B and noise. Using this information (16) can be expressed as (17) at the top of this page, where (a) follows by expressing the received signals for the Δ set in terms of their original components; (b) follows by removing the X^A parts since they have no effect on entropy and also removing the conditioning since X_k^B and Z are independent of W^A; (c) is obtained by replacing channel coefficients from BS B to user $a1$ with ones to cell B users, due to their statistical equivalence, and lastly (d) is obtained by representing the X^B and noise components in terms of the signals received at the corresponding inter-cell interference free cell B users. Finally considering all the components of the first negative entropy term in (17) to be independent of each other, we obtain a rate expression for $a1$ in terms of the separate entropy contributions of the received signals and E_{a1} as in (18). Following a similar process for users $a2$, $b1$ and $b2$ separately we obtain outer bounds on their achievable rates as in (19), (20) and (21). Further details on how to obtain these expressions are provided in Appendices B-I, B-II and B-III respectively.

Combining expressions (18) to (21) as $nR_{\Sigma(SB)} = nR_{a1} + nR_{a2} + nR_{b1} + nR_{b2}$, the achievable sum rate across the whole network is bounded as in (22) above. Next, we consider the remaining negative terms in (22) and pair one of $\{E_{a1}, E_{a2}, E_{b1}, E_{b2}\}$ with one of $\{h(Y_{15}^{a1}), h(Y_{16}^{a2}), h(Y_{14}^{b1}), h(Y_{13}^{b2})\}$ to find a joint lower bound. Starting with E_{a1}, we can express it as

$$
\begin{aligned}
E_{a1} &= h(Y_1^{a1}, Y_{16}^{a1} \mid W^A, Y_2^{a1},\ldots,Y_{15}^{a1}) \\
&= h(Y_{16}^{a1} \mid W^A, Y_2^{a1},\ldots,Y_{15}^{a1}) + h(Y_1^{a1} \mid W^A, Y_2^{a1},\ldots,Y_{16}^{a1}) \\
&\overset{(a)}{=} h(H_{a1,A}X_{16}^A + H_{a1,B}X_{16}^B + Z \mid W^A) \\
&\quad + \underbrace{h(Y_1^{a1} \mid W^A, Y_2^{a1},\ldots,Y_{16}^{a1})}_{\geq h(Y_1^{a1} \mid W^A, Y_2^{a1},\ldots,Y_{16}^{a1}, W^B) = no(\log P)} \\
&\overset{(b)}{\geq} h(H_{a1,B}X_{16}^B + Z) + no(\log P)
\end{aligned}
$$

where (a) follows by expressing Y_{16}^{a1} in terms of the original components and considering it to be independent of $Y_2^{a1},\ldots,Y_{15}^{a1}$, and (b) follows by neglecting the X^A component since its effect is negligible with respect to entropy and removing the conditioning since the remaining terms are independent of W^A. Pairing E_{a1} with $h(Y_{16}^{a2})$, we obtain

$$
\begin{aligned}
&h(Y_{16}^{a2}) + E_{a1} \\
&\overset{(a)}{\geq} h(H_{a2,A}X_{16}^A + Z) + h(H_{a1,B}X_{16}^B + Z) + no(\log P) \\
&\overset{(b)}{=} h(H_{a1,A}X_{16}^A) + h(H_{a1,B}X_{16}^B) + no(\log P)
\end{aligned} \tag{23}
$$

where (a) follows by representing Y_{16}^{a2} in terms of its original components, and (b) follows by applying the fact that $H_{a2,A}$ and $H_{a1,A}$ are statistically equivalent, and also by removing the noise components since their effect disappears with high SNR and can therefore be integrated in the $no(\log P)$ term.

$$\begin{aligned} nR_{\Sigma(SB)} \leq\, & h(Y_1^{a1}) + h(Y_2^{a1}) + h(Y_5^{a1}) + \cdots + h(Y_8^{a1}) + h(Y_{10}^{a1}) + h(Y_{12}^{a1}) + h(Y_{13}^{a1}) + h(Y_{14}^{a1}) + h(Y_1^{a2}) + h(Y_2^{a2}) \\ & + h(Y_4^{a2}) + h(Y_6^{a2}) + \cdots + h(Y_9^{a2}) + h(Y_{11}^{a2}) + h(Y_{13}^{a2}) + h(Y_{14}^{a2}) + h(Y_1^{b1}) + \cdots + h(Y_5^{b1}) + h(Y_7^{b1}) \\ & + h(Y_9^{b1}) + h(Y_{10}^{b1}) + h(Y_{15}^{b1}) + h(Y_{16}^{b1}) + h(Y_1^{b2}) + \cdots + h(Y_5^{b2}) + h(Y_8^{b2}) + h(Y_{11}^{b2}) + h(Y_{12}^{b2}) + h(Y_{15}^{b2}) \\ & + h(Y_{16}^{b2}) + no(\log P) + n\epsilon \\ \overset{(a)}{\leq}\, & n\,(\,2 + 2\lambda_1 + 2\lambda_2 + \lambda_4 + \lambda_5 + \lambda_7 + \lambda_8\,)(\log P) + no(\log P) + n\epsilon \end{aligned} \tag{29}$$

$$\begin{aligned} nR_{\Sigma(GA)} \leq\, & h(Y_1^{a1}, \ldots, Y_{16}^{a1}, Y_1^{a2}, \ldots, Y_{16}^{a2}, G^A) - \underbrace{h(Y_1^{a1}, \ldots, Y_{16}^{a1}, Y_1^{a2}, \ldots, Y_{16}^{a2}, G^A \mid W^A, W^B)}_{=no(\log P)} + n\epsilon \\ \leq\, & h(Y_1^{a1}) + \cdots + h(Y_{16}^{a1}) + h(Y_1^{a2}) + \cdots + h(Y_{16}^{a2}) + 2h(Y_2^B) + 2h(Y_3^B) + 2h(Y_4^B) + 2h(Y_5^B) \\ & + h(Y_7^B) + \cdots + h(Y_{12}^B) + h(Y_{15}^B) + h(Y_{16}^B) + no(\log P) + n\epsilon \\ \overset{(a)}{\leq}\, & n(\,2 + 2\lambda_2 + 2\lambda_3 + 2\lambda_4 + 2\lambda_5 + \lambda_7 + \lambda_8 + \lambda_9 + \lambda_{10} + \lambda_{11} + \lambda_{12} + \lambda_{15} + \lambda_{16}\,)(\log P) + no(\log P) + n\epsilon \end{aligned} \tag{32}$$

Additionally, considering $h(Y_{16}^{a1})$ and the fact that $Y_{16}^{a1} = H_{a1,A}X_{16}^A + H_{a1,B}X_{16}^B + Z$, applying Lemma 1 from Appendix C results in

$$h(Y_{16}^{a1}) \leq h(H_{a1,A}X_{16}^A) + h(H_{a1,B}X_{16}^B) + no(\log P). \tag{24}$$

Subtracting (23) from (24), we obtain

$$h(Y_{16}^{a1}) - h(Y_{16}^{a2}) - E_{a1} \leq no(\log P)\,. \tag{25}$$

Applying a similar process to different pairings we can also establish the following inequalities

$$h(Y_{15}^{a2}) - h(Y_{15}^{a1}) - E_{a2} \leq no(\log P), \tag{26}$$

$$h(Y_{13}^{b1}) - h(Y_{13}^{b2}) - E_{b1} \leq no(\log P), \tag{27}$$

$$h(Y_{14}^{b2}) - h(Y_{14}^{b1}) - E_{b2} \leq no(\log P). \tag{28}$$

Using (25) to (28) in the total rate expression (22) we obtain (29) at the top of this page, where (a) follows by using the fact that Gaussian distribution maximises differential entropy and applying $\sum_{k=1}^{16} \lambda_k = 1$. Finally, normalising by $n(\log P)$ and letting $P \to \infty$, we obtain the desired DoF sum bound as

$$d_{\Sigma(SB)} \leq\; 2 + 2\lambda_1 + 2\lambda_2 + \lambda_4 + \lambda_5 + \lambda_7 + \lambda_8\,. \tag{30}$$

B. Genie aided bounds

The genie aided bounds for the MISO/MIMO scenario are obtained in a similar way to the SISO ones from Section III-B. However, in this case the number of genies provided must ensure that 2 symbols from the other cell can be retrieved. Starting with the cell A genie aided DoF bound, we have

$$nR_{\Sigma(GA)} \leq I(W^A, W^B; Y_1^{a1}, \ldots, Y_{16}^{a1}, Y_1^{a2}, \ldots, Y_{16}^{a2}, G^A) + n\epsilon \tag{31}$$

where G^A represents the additional set of genies required such that cell B data may be reconstructed within cell A. The amount of genies required is either one or two, depending on the number of signals containing cell B information reaching cell A. Looking at all the possible topologies in Fig. 2, this corresponds to

$$G^A = \{2 \times [Y_2^B, Y_3^B, Y_4^B, Y_5^B], Y_7^B, \ldots, Y_{12}^B, Y_{15}^B, Y_{16}^B\}$$

where B represents either $b1$ or $b2$. Having defined G^A, this can be integrated into (31) to obtain (32) above where (a) follows by using the fact that Gaussian distribution maximises differential entropy and applying $\sum_{k=1}^{16} \lambda_k = 1$. Normalising by $n(\log P)$ and letting $P \to \infty$, results in

$$\begin{aligned} d_{\Sigma(GA)} \leq\, & 2 + 2\lambda_2 + 2\lambda_3 + 2\lambda_4 + 2\lambda_5 + \lambda_7 + \lambda_8 \\ & + \lambda_9 + \lambda_{10} + \lambda_{11} + \lambda_{12} + \lambda_{15} + \lambda_{16}\,. \end{aligned} \tag{33}$$

Following a similar process for cell B, details for which are provided in Appendix B-IV, we obtain

$$\begin{aligned} d_{\Sigma(GB)} \leq\, & 2 + 2\lambda_2 + \lambda_4 + \lambda_5 + 2\lambda_6 + 2\lambda_7 + 2\lambda_8 \\ & + \lambda_9 + \lambda_{10} + \lambda_{11} + \lambda_{12} + \lambda_{13} + \lambda_{14}\,. \end{aligned} \tag{34}$$

Finally, the result for $d_{\Sigma,M}$ in Theorem 2 is obtained by combining the separate bounds from (30), (33) and (34).

■

Remark 1: Some similarities can be observed between the IBC outer bounds in Theorems 1 and 2 and the one for the two-user SISO IC from [15]. This is expected since the IC is essentially a subset of the IBC having only one user per cell. Before drawing any similarities, we first need to express the outer bound from Theorem 1 in an alternative way as

$$d_{\Sigma,S} \leq 1 + \lambda_2 + \lambda_4 + \lambda_5 + \lambda_7 + \cdots + \lambda_{12} + \Psi \tag{35}$$

where

$$\Psi = \min\{\lambda_1 + \lambda_{13} + \cdots + \lambda_{16},\; \lambda_3 + \lambda_{15} + \lambda_{16},\; \lambda_6 + \lambda_{13} + \lambda_{14}\}.$$

This reformulated version of Theorem 1, alongside with the outer bound in Theorem 2 and the SISO IC result in [15] can collectively be summarised as $d_\Sigma \leq d_c + \lambda_\eta + \kappa$, where d_c is the achievable DoF per cell when no inter-cell interference is present. This is equal to 1 for the two-user SISO IC and the two-cell two-user-per-cell SISO IBC, and corresponds to 2 for the MISO/MIMO IBC counterpart. For all scenarios λ_η consists exclusively of the probability of occurrence of all the states that directly obtain higher DoF than the fully connected one; its fixed presence in the outer bound reflects the corresponding DoF gain. Finally κ depends on which bound is the most restrictive, but is always a function of the probability of occurrence of the states which inherently obtain less DoF than the inter-cell interference free one.

V. Achievable DoF for SISO IBC

Without knowledge of the network's topological structure, a fully connected scenario has to be assumed at all times, achieving a sum DoF of 1 across all states for the SISO system. However, if global topological CSIT is provided, the BSs can adapt their transmission strategies to exploit the partially connected states and obtain a DoF gain.

A. Single state has probability of occurrence equal to one

This is an extreme case for the scenario considered in this work, with $\lambda_i = 1$ and $\lambda_j = 0$ for $j = 1, \ldots, 16, j \neq i$. It essentially implies connectivity is fixed in state i throughout the whole transmission process.

For $i \in \{2, 4, 5, 7, \ldots, 12\}$ there is at least one user per cell that is free from inter-cell interference. These states represent the best case scenario from an achievable DoF perspective, with the outer bound in Theorem 1 corresponding to $d_{\Sigma,S} \leq 2$. Having knowledge of the network's structure, both BSs can operate simultaneously and serve one inter-cell interference free user per cell, achieving 2 DoF across the whole network. This is equal to the outer bound itself and corresponds to a two-fold increase over the no global topological CSIT case.

For the remaining states, $i \in \{1, 3, 6, 13, \ldots, 16\}$, at least one of the two cells has both users experiencing inter-cell interference and the outer bound from Theorem 1 corresponds to $d_{\Sigma,S} \leq 1$. Sum DoF of 1 can be achieved simply by operating one BS at a time and serving one user within the corresponding cell.

B. Arbitrary state probabilities

As mentioned earlier without global topological CSIT, only 1 DoF can be achieved regardless of the current connectivity state; however if this information is available, the BSs can use it to adapt their transmission strategy accordingly. Both BSs operate simultaneously for states where there is at least one inter-cell interference free user in each cell, delivering a symbol each to two users from different cells. For the remaining states, only one BS needs to be operated, delivering one symbol across the whole network. Therefore, considering all the states in Fig. 2 it is possible to obtain

$$\begin{aligned}\text{DoF} &= \begin{cases} 1 \text{ for states } 1, 3, 6, 13, 14, 15, 16 \\ 2 \text{ for states } 2, 4, 5, 7, 8, 9, 10, 11, 12 \end{cases}. \\ &= 1 + \lambda_2 + \lambda_4 + \lambda_5 + \lambda_7 + \cdots + \lambda_{12} \end{aligned} \tag{36}$$

Higher DoF can be achieved via joint coding across states. This was first applied to the two-user IC in [15] where the authors propose a scheme based on this principle to deliver 2 symbols across 3 states. Within our setting, joint coding can be used across a variety of different state combinations to deliver a total of 4 symbols over 3 states.

Considering the alternating connectivity states in Fig. 2, it can be noticed that the same interference links appear twice over states $\{3, 13, 14\}$. Thus the three states in this set can be combined together to resolve inter-cell interference. Defining s_r as the symbol intended for user r, then for scheme $\mathcal{S}_1$ which performs joint coding across states $\{3, 13, 14\}$, BSs transmit according to Table II. User $b2$ obtains s_{b2} directly from the signal received in state 13, while the combination of received signals at the remaining users allows for interference cancellation decoding. For users $a1$ and $a2$, received signals are functions of s_{a1}, s_{a2} and s_{b2}. Having three independent equations in terms of three different symbols, then the desired data can be obtained at the respective users. For user $b1$, all received signals are functions of $(s_{a1} + s_{a2})$, s_{b1} and s_{b2}. Considering $(s_{a1} + s_{a2})$ as a single symbol, we have three independent equations for three unknowns and can solve for s_{b1}. Therefore 1 symbol each is transmitted to all 4 users in 3 channel uses, leading to an average of $\frac{4}{3}$ DoF per state.

Joint coding can also be applied across other sets of states. In particular, states $\{6, 15, 16\}$ can be combined together using scheme $\mathcal{S}_2$ in Table III and states $\{1, 3, 6\}$ can be combined via scheme $\mathcal{S}_3$ in Table IV. In each case $\frac{4}{3}$ DoF per state are achieved. Additionally for quasi-static fading channels, where the value of the channel links does not change across the states involved in the scheme, it is also possible to code across states $\{13, 15, 16\}$ using scheme $\mathcal{S}_4$ in Table V or across states $\{14, 15, 16\}$ via scheme $\mathcal{S}_5$ in Table VI.

TABLE II: Transmission strategy for scheme $\mathcal{S}_1$.

Transmitted symbols	State 3	State 13	State 14
X^A	$(s_{a1} + s_{a2})$	$(s_{a1} + s_{a2})$	s_{a1}
X^B	s_{b1}	s_{b2}	s_{b2}

TABLE III: Transmission strategy for scheme $\mathcal{S}_2$.

Transmitted symbols	State 6	State 15	State 16
X^A	s_{a2}	s_{a1}	s_{a1}
X^B	$(s_{b1} + s_{b2})$	$(s_{b1} + s_{b2})$	s_{b1}

TABLE IV: Transmission strategy for scheme $\mathcal{S}_3$.

Transmitted symbols	State 1	State 3	State 6
X^A	$(s_{a1} + s_{a2})$	$(s_{a1} + s_{a2})$	s_{a1}
X^B	$(s_{b1} + s_{b2})$	s_{b1}	$(s_{b1} + s_{b2})$

TABLE V: Transmission strategy for scheme $\mathcal{S}_4$.

Transmitted symbols	State 13	State 15	State 16
X^A	$(s_{a1} + s_{a2})$	s_{a1}	s_{a2}
X^B	s_{b2}	s_{b1}	s_{b2}

TABLE VI: Transmission strategy for scheme $\mathcal{S}_5$.

Transmitted symbols	State 14	State 15	State 16
X^A	$(s_{a1} + s_{a2})$	s_{a1}	s_{a2}
X^B	s_{b1}	s_{b1}	s_{b2}

Due to the repetition of the states involved in schemes $\mathcal{S}_1$ to $\mathcal{S}_5$, no more than two can be combined together. The possible combinations are: $\mathcal{S}_1$ and $\mathcal{S}_2$, $\mathcal{S}_3$ and $\mathcal{S}_4$ or $\mathcal{S}_3$ and $\mathcal{S}_5$. With arbitrary state probabilities, achievable DoF for each combination can be characterised as follows.

(i) Schemes $\mathcal{S}_1$ and $\mathcal{S}_2$

$d_{\Sigma,S-\mathcal{S}_1,\mathcal{S}_2} = 1 + \lambda_2 + \lambda_4 + \lambda_5 + \lambda_7 + \cdots + \lambda_{12} + \alpha_1 + \beta_1$ where $\alpha_1 = \min\{\lambda_3, \lambda_{13}, \lambda_{14}\}$ and $\beta_1 = \min\{\lambda_6, \lambda_{15}, \lambda_{16}\}$.

(ii) Schemes $\mathcal{S}_3$ and $\mathcal{S}_4$

$d_{\Sigma,S-\mathcal{S}_3,\mathcal{S}_4} = 1 + \lambda_2 + \lambda_4 + \lambda_5 + \lambda_7 + \cdots + \lambda_{12} + \alpha_2 + \beta_2$ where $\alpha_2 = \min\{\lambda_1, \lambda_3, \lambda_6\}$ and $\beta_2 = \min\{\lambda_{13}, \lambda_{15}, \lambda_{16}\}$.

(iii) Schemes $\mathcal{S}_3$ and $\mathcal{S}_5$

$d_{\Sigma,S-\mathcal{S}_3,\mathcal{S}_5} = 1 + \lambda_2 + \lambda_4 + \lambda_5 + \lambda_7 + \cdots + \lambda_{12} + \alpha_2 + \beta_3$

where α_2 is as defined earlier and $\beta_3 = \min\{\lambda_{14}, \lambda_{15}, \lambda_{16}\}$.

Combining $d_{\Sigma,S-\mathcal{S}_1,\mathcal{S}_2}$, $d_{\Sigma,S-\mathcal{S}_3,\mathcal{S}_4}$ and $d_{\Sigma,S-\mathcal{S}_3,\mathcal{S}_5}$ into a single expression for the maximum achievable DoF, we obtain the following

$$d_{\Sigma,S-Ach} = 1 + \lambda_2 + \lambda_4 + \lambda_5 + \lambda_7 + \cdots + \lambda_{12} + \omega \quad (37)$$

where $\omega = \max\{\alpha_1 + \beta_1, \alpha_2 + \beta_2, \alpha_2 + \beta_3\}$ for quasi-static fading channels and $\omega = \alpha_1 + \beta_1$ for the fast-fading scenario.

Note that the only difference between the outer bound in Theorem 1 (see the reformulated expression in (35)) and the achievable DoF expression in (37) is the final term. In fact for any state probabilities such that $\omega = \Psi$, the two are equal, resulting in an outer bound which is achievable. For example this happens for $\lambda_1 = \lambda_3 = \lambda_6 = \lambda_{13} = \cdots = \lambda_{16} = 0$ and general values of λ_i where $i \in \mathcal{I} = \{2, 4, 5, 7, \ldots, 12\}$ and $\sum_{i\in\mathcal{I}} \lambda_i = 1$.

C. Equal state probabilities

When all states are equiprobable, i.e. $\lambda_1 = \cdots = \lambda_{16} = \frac{1}{16}$, using the result of Theorem 1 we can establish the following corollary.

Corollary 1: For the two-cell two-user-per-cell SISO IBC with alternating connectivity and equiprobable states, $d_{\Sigma,S} \leq 1\frac{3}{4}$.

Without global topological CSIT, only a sum DoF of 1 can be achieved. However if topological CSIT is available the DoF in (36) can be obtained; with equiprobable states this implies 25 symbols are transmitted in 16 channel uses on average, equivalent to $1\frac{9}{16}$ DoF. While this is an improvement of $\frac{9}{16}$ over the no global topological CSIT case, it is still $\frac{3}{16}$ DoF away from the outer bound in Corollary 1. Applying joint coding across states the DoF in (37) can be achieved. With equiprobable states this is equal to $1\frac{11}{16}$ and corresponds to a gain of $\frac{11}{16}$ DoF over the no global topological CSIT setting. While it does not correspond to the outer bound in Corollary 1, there is only a difference of $\frac{1}{16}$ between the two, i.e. 96.4% of the outer bound is achieved.

VI. Achievable DoF for MISO and MIMO IBC

In this section we investigate the achievability of the outer bound in Theorem 2. Without global topological CSIT, a fully connected network has to be assumed at all times. This allows only for one possible strategy where the BSs are given unique transmission opportunities, thereby achieving 2 DoF across all states. However, if global topological information is provided, the BSs can adapt their transmission strategies in order to exploit the partially connected states and achieve higher DoF.

A. Single state has probability of occurrence equal to one

This represents an extreme case for the scenario considered in this work, where connectivity is fixed in a single state throughout the whole transmission process, i.e. $\lambda_i = 1$ and $\lambda_j = 0$ for $j = 1, \ldots, 16, j \neq i$.

For $i = 2$, Theorem 2 can be represented as $d_{\Sigma,M} \leq 4$. From an achievable DoF perspective, this situation corresponds to the best case scenario since all users are inter-cell interference free. Having knowledge of the network's topology, both BSs can operate simultaneously and deliver a symbol each to their respective users, thereby achieving 4 DoF across the whole network. This is equal to the outer bound itself and corresponds to a two-fold increase in achievable DoF over the no global topological CSIT case.

For $i \in \{4, 5, 7, 8\}$, three out of the four users are free from inter-cell interference and the outer bound in Theorem 2 corresponds to $d_{\Sigma,M} \leq 3$. Since network topology is known, both BSs can operate simultaneously to serve the three inter-cell interference free users, while the fourth user is not served due to inter-cell interference. This achieves 3 DoF over the whole network, which is equal to the derived outer bound and provides a gain of 1 DoF over the case where global topological CSIT is not provided.

For the remaining states, $i \in \{1, 3, 6, 9, \ldots, 16\}$, the outer bound from Theorem 1 is $d_{\Sigma,M} \leq 2$. Sum DoF of 2 can be achieved simply by operating one BS at a time and delivering one symbol each to the two users in the corresponding cell.

B. Arbitrary state probabilities

Without global topological CSIT, only 2 DoF can be achieved regardless of the current connectivity state; however if this information is provided, the BSs can adapt their transmission strategies to exploit the partially connected states. Considering the set of states in Fig. 2, it is possible to achieve

$$\begin{aligned}\text{DoF} &= \begin{cases} 2 \text{ for states } 1, 3, 6, 9, 10, 11, 12, 13, 14, 15, 16 \\ 3 \text{ for states } 4, 5, 7, 8 \\ 4 \text{ for state } 2. \end{cases} \\ &= 2 + 2\lambda_2 + \lambda_4 + \lambda_5 + \lambda_7 + \lambda_8 \end{aligned} \quad (38)$$

Higher DoF can be obtained via scheme $\mathcal{S}_6$ which applies joint coding across states. Looking at the states in Fig. 2, it can be noticed that the interference links present in states 3 and 6 are contained within state 1; therefore state 1 can be used to resolve them. The transmission strategy for scheme $\mathcal{S}_6$ is outlined in Table VII.

TABLE VII: Transmission strategy for scheme $\mathcal{S}_6$.

Transmitted symbols	State 3	State 6	State 1
X^A	S_A	$\underline{S}_A$	S_A
X^B	S_B	$\underline{S}_B$	$\underline{S}_B$

For the MISO case, we define the signals transmitted from BS A as $S_A = (V_{a1}s_{a1} + V_{a2}s_{a2})$ and $\underline{S}_A = (\underline{V}_{a1}\underline{s}_{a1} + \underline{V}_{a2}\underline{s}_{a2})$, where V_i and $\underline{V}_i$ are $M \times 1$ ZF precoders. These are constructed using local CSIT knowledge, according to the orthogonality principles explained earlier in Section II and ensure that each user can extract the desired symbol from the combined signal transmitted by the corresponding BS. The symbols transmitted by BS B are defined in a similar manner. By following the transmission strategy in Table VII, signals received over the three states at users $a1$ and $a2$ consist only of S_A, $\underline{S}_A$ and $\underline{S}_B$, thus both users can decode for S_A and $\underline{S}_A$. Additionally due to the ZF precoding, users only see the desired part of the combined signal, thus a_1 obtains $\{s_{a1}, \underline{s}_{a1}\}$, while $a2$ obtains $\{s_{a2}, \underline{s}_{a2}\}$. A similar decoding process is carried out at users $b1$ and $b2$ to obtain $\{s_{b1}, \underline{s}_{b1}\}$ and $\{s_{b2}, \underline{s}_{b2}\}$ respectively. Therefore across the 3 states a total of 8 new symbols are delivered, 2 for each user.

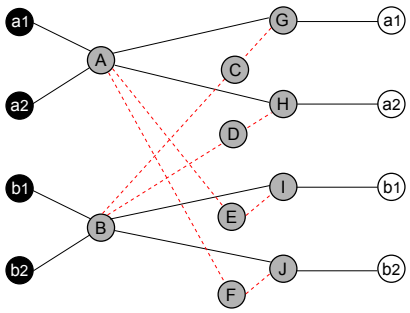

(a) Wired equivalent for SISO scenario

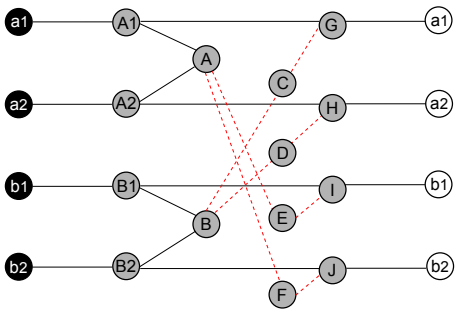

(b) Wired equivalent for MISO/MIMO scenario

Fig. 5: Examples of wired network equivalents for the wireless scenarios considered in this work. Sources are in black, destinations are in white and intermediate nodes are in grey. For wired networks connectivity can change due to variations in the linear network coding coefficients. Both figures represent the fully connected state, i.e. state 1 in Fig. 2. The presence of the dotted red lines is variable depending on the value of the corresponding network coding coefficients and reflects the alternating connectivity.

For the MIMO case, we define the signals transmitted from BS A as $S_A = (V_{a1}s_{a1} + V_{a2}s_{a2})$ and $\underline{S}_A = (V_{a1}\underline{s}_{a1} + \underline{V}_{a2}\underline{s}_{a2})$. V_i and $\underline{V}_i$ are $M \times 1$ precoders which change for every state involved in scheme $\mathcal{S}_6$ and can be considered as being pseudo-random; they would normally be used to enforce transmit power constraints, which is inconsequential from a DoF perspective. The symbols transmitted by BS B are similarly defined. Considering users $a1$ and $a2$, it can be seen that across the whole set of states, received signals consist only of s_{a1}, s_{a2}, $\underline{s}_{a1}$, $\underline{s}_{a2}$, $\underline{s}_{b1}$ and $\underline{s}_{b2}$. Due to the multiple antenna configuration at the transmitters and receivers, both users $a1$ and $a2$ are in possession of six independent observations (two from each state) and can thus decode for their desired symbols, $\{s_{a1}, \underline{s}_{a1}\}$ and $\{s_{a2}, \underline{s}_{a2}\}$ respectively. A similar decoding process is carried out at users $b1$ and $b2$ to obtain $\{s_{b1}, \underline{s}_{b1}\}$ and $\{s_{b2}, \underline{s}_{b2}\}$ respectively. Therefore, by applying this scheme, each user obtains 2 new symbols across 3 states.

Using scheme $\mathcal{S}_6$, for arbitrary state probabilities, achievable DoF can be characterised as

$$d_{\Sigma,M-Ach} = 2 + 2\lambda_2 + \lambda_4 + \lambda_5 + \lambda_7 + \lambda_8 + \gamma \qquad (39)$$

where $\gamma = \min\{2\lambda_1, 2\lambda_3, 2\lambda_6\}$.

Notice the similarity between the achievable DoF in (39) and the outer bound in Theorem 2. The only difference is in the final term, such that for any state probabilities that result in $\gamma = \Phi$, the two are equal resulting in a tight outer bound. For example, this occurs when $\lambda_1 \leq \min\{\lambda_3, \lambda_6\}$ for arbitrary values of λ_k $\forall k = 1, \ldots, 16$.

C. Equal state probabilities

When all states are equiprobable, i.e. $\lambda_1 = \cdots = \lambda_{16} = \frac{1}{16}$, the result in Theorem 2 can be used to establish the following corollary.

Corollary 2: For the two-cell two-user-per-cell MISO/MIMO IBC with alternating connectivity and equiprobable states, where intra-cell interference is handled via spatial multiplexing, $d_{\Sigma,M} \leq 2\frac{1}{2}$.

Without global topological CSIT, only a sum DoF of 2 can be achieved. However if topological CSIT is available, the DoF in (38) can be obtained; with equiprobable states this is equivalent to $2\frac{3}{8}$ DoF, since 38 symbols are transmitted in 16 channel uses on average. While this is an improvement of $\frac{3}{8}$ DoF over the no global topological CSIT case, it is still $\frac{1}{8}$ DoF away from the outer bound value established in Corollary 2. Applying joint coding across states the DoF in (39) can be achieved. With equiprobable states this results in $2\frac{1}{2}$ DoF, which corresponds to a gain of $\frac{1}{2}$ DoF over the no global topological CSIT setting and is equal to the outer bound value from Corollary 2.

VII. Applicability of Derived Bounds to Wired Network Equivalents

It was recently established in [13] that under the topological interference management framework, the capacity of a wireless network and the corresponding wired instance are equivalent in their normalised forms; where the term 'corresponding' implies that the two networks have the same underlying noiseless linear network structure. For wireless networks, normalised capacity represents the achievable rate normalised by $\log(\text{SNR})$ as $\text{SNR} \to \infty$, i.e. DoF. For wired networks, normalised capacity refers to the capacity of the network divided by the capacity of a single link i.e. divided by $\log|\mathbb{GF}|$, where $\mathbb{GF}$ represents the finite Galois field.

This equivalence essentially implies that all networks (either wired or wireless) with the same logical end-to-end topology have the same normalised capacity, and requires wired networks to be SISO ones where each source has only one outgoing edge and each destination has only one incoming edge. Both wireless scenarios considered in this work can be mapped to such wired equivalent networks, an example of which is shown in Fig. 5, therefore from the results of Theorems 1 and and 2 we can establish the following corollaries.

Corollary 3: The normalised sum capacity of a wired network with the same end-to-end topology as the wireless SISO network considered in this work is upper bounded by $2 - \Theta$, where Θ is defined as in (3).

Corollary 4: The normalised sum capacity of a wired network with the same end-to-end topology as the wireless MISO/MIMO network considered in this work is upper bounded by $2 + 2\lambda_2 + \lambda_4 + \lambda_5 + \lambda_7 + \lambda_8 + \Phi$, where Φ is defined as in (15).

The bounds in these corollaries have also been confirmed by deriving the outer bounds for the wired scenarios, i.e. using discrete rather than differential entropy and omitting noise considerations. Details are not provided here, since our main focus is on the wireless case.

VIII. Conclusion

In this work we study the DoF of a two-cell two-user-per-cell IBC with alternating connectivity and global topological interference management. Our analysis is first carried out for SISO systems, and later extended to MISO and MIMO ones. For each setting, we derive novel DoF outer bounds and investigate their achievability. We also propose new transmission schemes based on joint coding across states and show under what conditions the derived outer bounds are achievable. In particular, when a single state has a probability of occurrence equal to one, the bounds are shown to be tight and for the best case scenario there is a two-fold increase in achievable DoF over the no global topological CSIT case. Additionally, when all states are equiprobable, the SISO system obtains a gain of $\frac{11}{16}$ DoF and achieves 96.4% of the derived outer bound. For the corresponding MISO/MIMO scenario, there is a gain of $\frac{1}{2}$ DoF and the outer bound itself can be achieved. Our results clearly show that significant DoF gains can be achieved when transmitters are provided with global topological information, indicating that even such a minimal level of global CSIT is still highly useful.

Appendix A
Additional details for proof of Theorem 1

I. Derivation of cell B rate outer bound in (8)

Considering the cell B achievable rate, we have

$$\begin{aligned} nR_B &\le I(W^B; Y_1^V, \dots, Y_{16}^V) + n\epsilon \\ &\overset{(a)}{=} h(Y_1^V, \dots, Y_{16}^V) - h(Y_Q^V, Y_R^V, Y_S^V, Y_T^V \,|\, W^B) + n\epsilon \\ &= h(Y_1^V, \dots, Y_{16}^V) - h(Y_R^V, Y_S^V, Y_T^V \mid W^B) \\ &\quad - \underbrace{h(Y_Q^V, \mid W^B, Y_R^V, Y_S^V, Y_T^V)}_{\ge H(Y_Q^V, \mid W^B, Y_R^V, Y_S^V, Y_T^V, W^A) = no(\log P)} + n\epsilon \\ &\le h(Y_1^V, \dots, Y_{16}^V) \\ &\quad - h(Y_R^V, Y_S^V, Y_T^V \mid W^B) + no(\log P) + n\epsilon \qquad (40) \end{aligned}$$

where (a) follows since the original set of 16 states is contained in states Q, R, S and T.

Considering (40) and the state configurations in Fig. 4, it can be noticed that the cell B received signals in states R and T consists only of an X^B component and noise. The X^B component has no effect on entropy and the effect of noise can be integrated in the $no(\log P)$ term. For all states corresponding to S, the cell B received signals are a combination of X^A, X^B and noise. The X^B component is negligible with respect to entropy. The X^A and noise components are independent of W^B and, due to the statistical equivalence of $H_{V,A}$ and $H_{U,A}$, can be represented in terms of the signal received at user U, provided that U is free from inter-cell interference. Comparing the list of S states from Table I, this is guaranteed as being always possible regardless of the current (U, V) combination only for state 3. Using this information we can express (40) as

$$nR_B \le h(Y_1^V, \dots, Y_{16}^V) - h(H_{U,A} X_3^A + Z) + no(\log P) + n\epsilon$$

which is equivalent to (8), since $Y_3^U = H_{U,A} X_3^A + Z$.

II. Derivation of cell B genie aided DoF bound in (14)

The genie aided bound for the cell B achievable rate, is given by

$$nR_{\Sigma(GB)} \le I(W^A, W^B; Y_1^V, \dots, Y_{16}^V, G^B) + n\epsilon \qquad (41)$$

where G^B represents the genie set required at cell B such that the data required across the two cells can be decoded within cell B. Genies are necessary for all original states corresponding to states R and T, resulting in $G^B = \{Y_2^U, Y_4^U, \dots, Y_{14}^U\}$. Integrating G^B into (41), we obtain

$$\begin{aligned} nR_{\Sigma(GB)} &\le h(Y_1^V, \dots, Y_{16}^V, G^B) \\ &\quad - \underbrace{h(Y_1^V, \dots, Y_{16}^V, G^B \mid W^A, W^B)}_{= no(\log P)} + n\epsilon \\ &\le h(Y_1^V) + \dots + h(Y_{16}^V) + h(Y_2^U) \\ &\quad + h(Y_4^U) + \dots + h(Y_{14}^U) + no(\log P) + n\epsilon \\ &\overset{(a)}{\le} n(2 - \lambda_1 - \lambda_3 - \lambda_{15} - \lambda_{16}) + no(\log P) + n\epsilon \end{aligned}$$

where (a) follows from the fact that Gaussian distribution maximises differential entropy and using $\sum_{k=1}^{16} \lambda_k = 1$. Normalising by $n(\log P)$ and letting $P \to \infty$, we obtain the cell B genie aided DoF bound in (14).

Appendix B
Additional details for proof of Theorem 2

I. Derivation of user $a2$ achievable rate bound in (19)

For user $a2$, we have

$$\begin{aligned} nR_{a2} &\le I(W^A; Y_1^{a2}, \dots, Y_{16}^{a2}) + n\epsilon \\ &= h(Y_1^{a2}, \dots, Y_{16}^{a2}) - h(Y_1^{a2}, \dots, Y_{16}^{a2} \mid W^A) + n\epsilon \\ &= h(Y_1^{a2}, \dots, Y_{16}^{a2}) - h(Y_{\Omega'}^{a2}, Y_{\Omega}^{a2} \mid W^A) \\ &\quad - \underbrace{h(Y_1^{a2}, Y_{15}^{a2} \mid W^A, Y_2^{a2}, \dots, Y_{14}^{a2}, Y_{16}^{a2})}_{= E_{a2}} + n\epsilon \qquad (42) \end{aligned}$$

where $\Omega' = \{2,3,4,5,8,10,12,16\}$ and $\Omega = \{6,7,9,11,13,14\}$.

For the Ω' set, the $a2$ received signal consists only of an X^A component, which has no effect on entropy, and noise whose contribution is $no(\log P)$. For the Ω set, data received at $a2$ is a combination of X^A, X^B and noise. The X^A component can be ignored since it is a function of W^A; while the X^B and noise components can be represented using signals received at inter-cell interference free cell B users, due to their statistical equivalence. Using this information (42) can be expressed as (43) at the top of the following page. Finally, by considering all the components of the first negative term in (43) to be independent of each other, we obtain (19).

$$nR_{a2} \leq h(Y_1^{a2},\ldots,Y_{16}^{a2}) - h(H_{b1,B}X_6^B+Z, H_{b2,B}X_7^B+Z, H_{b2,B}X_9^B+Z, H_{b1,B}X_{11}^B+Z, H_{b2,B}X_{13}^B+Z, H_{b1,B}X_{14}^B+Z) - E_{a2} + no(\log P) + n\epsilon \;=\; h(Y_1^{a2},\ldots,Y_{16}^{a2}) - h(Y_6^{b1},Y_7^{b2},Y_9^{b2},Y_{11}^{b1},Y_{13}^{b2},Y_{14}^{b1}) - E_{a2} + no(\log P) + n\epsilon \quad (43)$$

$$nR_{b1} \leq h(Y_1^{b1},\ldots,Y_{16}^{b1}) - h(H_{a1,A}X_3^A+Z, H_{a1,A}X_4^A+Z, H_{a1,A}X_9^A+Z, H_{a2,A}X_{10}^A+Z, H_{a1,A}X_{15}^A+Z, H_{a2,A}X_{16}^A+Z) - E_{b1} + no(\log P) + n\epsilon \;=\; h(Y_1^{b1},\ldots,Y_{16}^{b1}) - h(Y_3^{a1},Y_4^{a1},Y_9^{a1},Y_{10}^{a2},Y_{15}^{a1},Y_{16}^{a2}) - E_{b1} + no(\log P) + n\epsilon \quad (45)$$

$$nR_{b2} \leq h(Y_1^{b2},\ldots,Y_{16}^{b2}) - h(H_{a2,A}X_3^A+Z, H_{a2,A}X_5^A+Z, H_{a1,B}X_{11}^A+Z, H_{a2,B}X_{12}^A+Z, H_{a1,B}X_{15}^A+Z, H_{a2,B}X_{16}^A+Z) - E_{b2} + no(\log P) + n\epsilon \;=\; h(Y_1^{b2},\ldots,Y_{16}^{b2}) - h(Y_3^{a2},Y_5^{a2},Y_{11}^{a1},Y_{12}^{a2},Y_{15}^{a1},Y_{16}^{a2}) - E_{b2} + no(\log P) + n\epsilon \quad (47)$$

$$\begin{aligned} nR_{\Sigma(GB)} &\leq h(Y_{16}^{b1},\ldots,Y_{16}^{b1},Y_1^{b2},\ldots,Y_{16}^{b2},G^B) - \underbrace{h(Y_{16}^{b1},Y_1^{b2},\ldots,Y_{16}^{b2},G^B \mid W^A,W^B)}_{=no(\log P)} + n\epsilon \\ &\leq h(Y_1^{b1}) + \cdots + h(Y_{16}^{b1}) + h(Y_1^{b2}) + \cdots + h(Y_{16}^{b2}) + 2h(Y_2^A) + h(Y_4^A) + h(Y_5^A) + 2h(Y_6^A) + 2h(Y_7^A) + 2h(Y_8^A) \\ &\quad + h(Y_9^A) + \cdots + h(Y_{14}^A) + no(\log P) + n\epsilon \\ &\overset{(a)}{\leq} n\,(\,2 + 2\lambda_2 + \lambda_4 + \lambda_5 + 2\lambda_6 + 2\lambda_7 + 2\lambda_8 + \lambda_9 + \cdots + \lambda_{14}\,)(\log P) + no(\log P) + n\epsilon \end{aligned} \quad (49)$$

II. Derivation of user $b1$ achievable rate bound in (20)

For user $b1$, we have

$$\begin{aligned} nR_{b1} &\leq I(W^B; Y_1^{b1},\ldots,Y_{16}^{b1}) + n\epsilon \\ &= h(Y_1^{b1},\ldots,Y_{16}^{b1}) - h(Y_1^{b1},\ldots,Y_{16}^{b1} \mid W^B) + n\epsilon \\ &= h(Y_1^{b1},\ldots,Y_{16}^{b1}) - h(Y_{\Gamma'}^{b1}, Y_{\Gamma}^{b1} \mid W^B) \\ &\quad - \underbrace{h(Y_1^{b1}, Y_{13}^{b1} \,|\, W^B, Y_2^{b1},\ldots,Y_{12}^{b1}, Y_{14}^{b1}, Y_{15}^{b1}, Y_{16}^{b1})}_{=E_{b1}} + n\epsilon \end{aligned} \quad (44)$$

where $\Gamma' = \{2,5,6,7,8,11,12,14\}$ and $\Gamma = \{3,4,9,10,15,16\}$.

For the Γ' set, the signal received at $b1$ consists only of an X^B component which has no effect on entropy, and noise whose contribution is $no(\log P)$. For the Γ set, the signals received at $b1$ consist of X^A, X^B and noise. The X^B component is a function of W^B and is therefore negligible with respect to entropy. The X^A and noise components can be expressed in terms of signals received at inter-cell interference free cell A users due to their statistical equivalence. This allows us to express (44) as (45) at the top of this page. Finally, (20) is obtained by considering all the components of the first negative term in (45) to be independent of each other.

III. Derivation of user $b2$ achievable rate bound in (21)

For user $b2$, we have

$$\begin{aligned} nR_{b2} &\leq I(W^B; Y_1^{b2},\ldots,Y_{16}^{b2}) + n\epsilon \\ &= h(Y_1^{b2},\ldots,Y_{16}^{b2}) - h(Y_1^{b2},\ldots,Y_{16}^{b2} \mid W^B) + n\epsilon \\ &= h(Y_1^{b2},\ldots,Y_{16}^{b2}) - h(Y_{\Upsilon'}^{b2}, Y_{\Upsilon}^{b2} \mid W^B) \\ &\quad - \underbrace{h(Y_1^{b2}, Y_{14}^{b2} \,|\, W^B, Y_2^{b2},\ldots,Y_{13}^{b2}, Y_{15}^{b2}, Y_{16}^{b2})}_{=E_{b2}} + n\epsilon \end{aligned} \quad (46)$$

where $\Upsilon' = \{2,4,6,7,8,9,10,13\}$ and $\Upsilon = \{3,5,11,12,15,16\}$.

For the Υ' set, the signal received at $b2$ consists only of an X^B component which has no effect on entropy, and noise whose contribution is $no(\log P)$. On the other hand for the Υ set, the data received at $b2$ consists of X^A, X^B and noise. The X^B component can be ignored, since it is solely a function of W^B. The X^A and noise components can be expressed in terms of the signals received at cell A users, due to their statistical equivalence. This allows us to express (46) as (47) at the top of this page. Finally, by considering all the components of the first negative entropy term in (47) to be independent of each other, we obtain (21).

IV. Derivation of cell B genie aided DoF bound in (34)

The genie aided bound for the cell B achievable rate, is given by

$$nR_{\Sigma(GB)} \leq I(W^A, W^B; Y_1^{b1},\ldots,Y_{16}^{b1}, Y_1^{b2},\ldots,Y_{16}^{b2}, G^B) + n\epsilon \quad (48)$$

where $G^B = \{2 \times [Y_2^A, Y_6^A, Y_7^A, Y_8^A], Y_4^A, Y_5^A, Y_9^A, \ldots, Y_{14}^A\}$ and represents the genie set required so that cell B is able to decode the data across both cells. Having defined G_B , this can be integrated into (48) to obtain (49) at the top of this page, where (a) follows by using the fact that Gaussian distribution maximises differential entropy and applying $\sum_{k=1}^{16} \lambda_k = 1$. Normalising by $n(\log P)$ and letting $P \to \infty$, we obtain the cell B genie aided DoF bound in (34).

APPENDIX C
USEFUL LEMMA

Lemma 1: For independent $H_{r,A}X_k^A$, $H_{r,B}X_k^B$ and Z, $h(H_{r,A}X_k^A + H_{r,B}X_k^B + Z) \leq h(H_{r,A}X_k^A) + h(H_{r,B}X_k^B) + no(\log P)$.

Proof: Starting with the following equality [21], for D and F independent of each other

$$\begin{aligned} h(D) + h(F) &= h(D,F) = h(D, D+F) \\ &= h(D+F) + h(F|D+F)\,. \end{aligned}$$

Letting $D = H_{r,A}X_k^A$ and $F = H_{r,B}X_k^B + Z$, we have

$$\begin{aligned} &h(H_{r,A}X_k^A + H_{r,B}X_k^B + Z) \\ &\quad = h(H_{r,A}X_k^A) + h(H_{r,B}X_k^B + Z) \\ &\quad\quad - \underbrace{h(H_{r,B}X_k^B + Z | H_{r,A}X_k^A + H_{r,B}X_k^B + Z)}_{\substack{\geq h(H_{r,B}X_k^B + Z | H_{r,A}X_k^A + H_{r,B}X_k^B + Z, W^B) \\ = h(Z | H_{r,A}X_k^A + H_{r,B}X_k^B + Z, W^B) = no(\log P)}} \end{aligned}$$

$$\overset{(a)}{\leq} h(H_{r,A}X_k^A) + h(H_{r,B}X_k^B) + no(\log P)$$

where (a) follows since the effect of noise disappears as $P \to \infty$ and can thus be represented as $no(\log P)$. ■

REFERENCES

[1] V. R. Cadambe and S. A. Jafar, "Interference alignment and degrees of freedom of the K-User interference channel," *IEEE Trans. Inf. Theory*, vol. 54, no. 8, pp. 3425-3441, Aug. 2008.

[2] B. Nazer, M. Gastpar, S. A. Jafar, and S. Vishwanath, "Ergodic interference alignment," *IEEE Trans. Inf. Theory*, vol. 58, no. 10, pp. 6355-6371, Oct. 2012.

[3] S. A. Jafar, "Blind interference alignment," *IEEE J. Sel. Topics Signal Process.*, vol. 6, no. 3, pp. 216-227, Jun. 2012.

[4] T. Gou, C. Wang, and S. A. Jafar, "Aiming perfectly in the dark - blind interference alignment through staggered antenna switching," *IEEE Trans. Signal Process.*, vol. 59, no. 6, pp. 2734-2744, Jun. 2011.

[5] T. Gou, S. A. Jafar, and C. Wang, "On the degrees of freedom of finite state compound wireless networks," *IEEE Trans. Inf. Theory*, vol. 57, no. 6, pp. 3286-3308, Jun. 2011.

[6] M.A. Maddah-Ali and D. Tse, "Completely stale transmitter channel state information is still very useful," *IEEE Trans. Inf. Theory*, vol. 58, no. 7, pp. 4418-4431, Jul. 2012.

[7] H. Maleki, S. A. Jafar, and S. Shamai, "Retrospective interference alignment over interference networks," *IEEE J. Sel. Topics Signal Process.*, vol. 6, no. 3, pp. 228-240, Jun. 2012.

[8] T. Gou and S. A. Jafar, "Optimal use of current and outdated channel state information: degrees of freedom of the MISO BC with mixed CSIT," *IEEE Commun. Lett.*, vol. 16, no. 7, pp. 1084-1087, Jul. 2012.

[9] S. Yang, M. Kobayashi, D. Gesbert, and X. Yi, "Degrees of freedom of time correlated MISO broadcast channel with delayed CSIT," *IEEE Trans. Inf. Theory*, vol. 59, no. 1, pp. 315-328, Jan. 2013.

[10] R. Tandon, S. A. Jafar, S. Shamai, and H. V. Poor, "On the synergistic benefits of alternating CSIT for the MISO broadcast channel," *IEEE Trans. Inf. Theory*, vol. 59, no. 7, pp. 4106-4128, Jul. 2013.

[11] P. de Kerret and D. Gesbert, "Interference alignment with incomplete CSIT sharing," *IEEE Trans. Wireless Commun.*, vol. 13, no. 5, pp. 2563-2573, May 2014.

[12] V. Aggarwal, A. S. Avestimehr, and A. Sabharwal, "On achieving local view capacity via maximal independent graph scheduling," *IEEE Trans. Inf. Theory*, vol. 57, no. 5, pp. 2711-2729, May 2011.

[13] S. A. Jafar, "Topological interference management through index coding," *IEEE Trans. Inf. Theory*, vol. 60, no. 1, pp. 529-568, Jan. 2014.

[14] X. Yi and D. Gesbert, "Topological interference management with transmitter cooperation," *IEEE Trans. Inf. Theory*, vol. 61, no. 11, pp. 6107-6130, Nov. 2015.

[15] H. Sun, C. Geng, and S.A Jafar, "Topological interference management with alternating connectivity," in *Proc. IEEE ISIT*, Jul. 2013, pp. 399-403.

[16] S. Gherekhloo, S. Chaaban, and A. Sezgin, "Topological interference management with alternating connectivity: the Wyner-type three user interference channel," in *Proc. IEEE IZS*, Feb. 2014.

[17] S. Gherekhloo, S. Chaaban, and A. Sezgin, "Resolving entanglements in topological interference management with alternating connectivity," in *Proc. IEEE ISIT*, Jun. 2014, pp. 1772-1776.

[18] W. Zhao, X. Ming, W. Chao, and M. Skoglund, "Degrees of freedom of two-hop MISO broadcast networks with mixed CSIT," *IEEE Trans. Wireless Commun.*, vol. 13, no. 12, pp. 6982-6995, Dec. 2014.

[19] H. Weingarten, Y. Steinberg, and S. Shamai, "The capacity region of the Gaussian multiple-input multiple-output broadcast channel," *IEEE Trans. Inf. Theory*, vol. 52, no. 9, pp. 3936-3964, Sep. 2006.

[20] C. Huang, S. A. Jafar, S. Shamai, and S. Vishwanath, "On degrees of freedom region of MIMO networks without channel state information at transmitters," *IEEE Trans. Inf. Theory*, vol. 58, no. 2, pp. 849-857, Feb. 2012.

[21] I. Kontoyiannis and M. Madiman, "Sumset and inverse sumset inequalities for differential entropy and mutual information," *IEEE Trans. Inf. Theory*, vol. 60, no. 8, pp. 4503-4514, Aug. 2014.

Paula Aquilina (S'14) received her B.Eng.(Hons.) degree in Electrical Engineering from the University of Malta in 2010 and an M.Sc. in Signal Processing and Communications from the University of Edinburgh in 2013. She is currently a Ph.D. candidate at the University of Edinburgh's Institute for Digital Communications. Her main area of research is wireless communications, with particular focus on interference management and network information theory.

Tharmalingam Ratnarajah (A'96-M'05-SM'05) is currently with the Institute for Digital Communications, University of Edinburgh, Edinburgh, UK, as a Professor in Digital Communications and Signal Processing. His research interests include signal processing and information theoretic aspects of 5G wireless networks, full-duplex radio, mmWave communications, random matrices theory, interference alignment, statistical and array signal processing and quantum information theory. He has published over 270 publications in these areas and holds four U.S. patents. He is currently the coordinator of the FP7 projects HARP (3.2M) in the area of highly distributed MIMO and ADEL (3.7M) in the area of licensed shared access. Previously, he was the coordinator of FP7 Future and Emerging Technologies project CROWN (2.3M) in the area of cognitive radio networks and HIATUS (2.7M) in the area of interference alignment. Dr. Ratnarajah is a Fellow of Higher Education Academy (FHEA), U.K., and an associate editor of the IEEE Transactions on Signal Processing.